

MAXI observations of long X-ray bursts

Motoko SERINO¹, Wataru IWAKIRI¹, Toru TAMAGAWA², Takanori
SAKAMOTO³, Satoshi NAKAHIRA⁴, Masaru MATSUOKA¹, Kazutaka
YAMAOKA^{5,6} and Hitoshi NEGORO⁷

¹MAXI team, RIKEN, 2-1 Hirosawa, Wako, Saitama 351-0198, Japan

²Nishina Center, RIKEN, 2-1 Hirosawa, Wako, Saitama 351-0198, Japan

³Department of Physics and Mathematics, Aoyama Gakuin University,
5-10-1 Fuchinobe, Chuo-ku, Sagami-hara, Kanagawa 252-5258

⁴JEM Mission Operations and Integration Center, Human Spaceflight Technology Directorate,
Japan Aerospace Exploration Agency, 2-1-1 Sengen, Tsukuba, Ibaraki 305-8505, Japan

⁵Department of Particle Physics and Astronomy, Nagoya University, Furo-cho, Chikusa-ku,
Nagoya, Aichi 464-8601, Japan

⁶Solar-Terrestrial Environment Laboratory, Nagoya University, Furo-cho, Chikusa-ku, Nagoya,
Aichi 464-8601, Japan

⁷Department of Physics, Nihon University, 1-8-14 Kanda-Surugadai, Chiyoda-ku, Tokyo
101-8308, Japan

*E-mail: motoko@crab.riken.jp

Received ; Accepted

Abstract

We report nine long X-ray bursts from neutron stars, detected with Monitor of All-sky X-ray Image (MAXI). Some of these bursts lasted for hours, and hence are qualified as superbursts, which are prolonged thermonuclear flashes on neutron stars and are relatively rare events. MAXI observes roughly 85% of the whole sky every 92 minutes in the 2–20 keV energy band, and has detected nine bursts with a long e-folding decay time, ranging from 0.27 to 5.2 hours, since its launch in 2009 August until 2015 August. The majority of the nine events were found to originate from transient X-ray sources. The persistent luminosities of the sources, when these prolonged bursts were observed, were lower than 1% of the Eddington luminosity for five of them and lower than 20% for the rest. This trend is contrastive to the 18 superbursts observed before MAXI, all but two of which originated from bright persistent sources. The distribution of the total emitted energy, i.e., the product of e-folding time and luminosity, of these bursts clusters around 10^{41} – 10^{42} erg, whereas either of the e-folding time and luminosity ranges for an order of magnitude. Among the nine events, two were from 4U 1850–086 during the phases of relatively low persistent-flux, whereas it usually exhibits standard short X-ray bursts during outbursts.

Key words: stars: neutron — X-rays: bursts — catalogs

1 Introduction

Since the discovery of a prolonged thermonuclear X-ray burst with the duration of several hours from 4U 1735–44 (Cornelisse et al. 2000), about 24 of such bursts, referred to

as “superbursts” (Wijnands 2001), have been reported from 14 sources (Keek et al. 2012; Negoro et al. 2012; Serino et al. 2014b). Among those, more than one superburst have been observed from 4U 1636–536, GX 17+2, and Ser X-1 (Wijnands

2001; Kuulkers et al. 2004; Kuulkers 2009). The shortest observed recurrence time of superbursts was only 8 days in GX 17+2 (in’t Zand et al. 2004).

Superbursts are considered to be thermonuclear flashes on neutron stars in low-mass X-ray binaries, and are similar to “normal” type-I X-ray bursts with a shorter duration. In fact, all the superburst sources are known to be (normal) X-ray burst sources. The primary difference between normal and superbursts is the duration. There is also a class of X-ray bursts with “intermediate duration” (Cumming et al. 2006), which have the decay time ranging from a hundred to a thousand seconds (Falanga et al. 2008). It is thought that the duration of an X-ray burst is related to the depth of the ignition point and the composition of the fuel. Superbursts are ignited by carbon burning deep in an ocean of heavier elements on a neutron star (Cumming & Bildsten 2001). On the other hand, intermediate-duration bursts are ignited by a thick layer of helium, which is most commonly provided by a degenerate companion star (in’t Zand et al. 2005; Falanga et al. 2008).

The composition of the fuel depends on the mass accretion rate. The relation between the accretion rate and the time scale of the burst has been studied for decades (e.g. Fujimoto et al. 1981 for normal bursts). Empirically, superbursts occurred on the persistent (not transient) sources with a high luminosity ($>10\%$ of the Eddington luminosity) (Kuulkers 2004; in’t Zand et al. 2004), whereas intermediate-duration bursts can occur in the sources with a very low luminosity ($<1\%$ of the Eddington luminosity) (in’t Zand et al. 2005; Falanga et al. 2008).

However, it is now understood that superbursts can occur in transient sources and persistent sources with a low luminosity (Chenevez et al. 2011; Asada et al. 2011; Serino et al. 2012; Serino et al. 2014b). For example, a superburst was observed from a transient source, 4U 1608–522 (Keek et al. 2008). The superburst occurred during an outburst, which had started 57.6 days before the burst. Keek et al. argued that the fuel of the superburst accumulated during the outburst was not sufficient to generate the released energy in the burst. 4U 1608–522 had shown multiple outbursts before the superburst. Keek et al. concluded that the fuel should have been accumulated during the preceding multiple outbursts. Another example is 4U 0614+091, a source with a low persistent luminosity ($<1\%$ of Eddington limit), from which a superburst has been detected on 2005 March 12 (MJD 53441) (Kuulkers et al. 2010). Although intermediate-duration bursts from 4U 0614+091 had been detected, superbursts from such a low-luminosity source had not been observed before that event. These discoveries presented serious problems in theoretical models of superburst ignition (Altamirano et al. 2012).

The Gas Slit Camera (GSC; Mihara et al. 2011b) onboard Monitor of All-sky X-ray Image (MAXI; Matsuoka et al. 2009) observes about 85% of the whole sky every 92 minutes

(Sugizaki et al. 2011), and has the capability of detecting transient events with the detection limit of $\sim 2 \times 10^{-9}$ erg cm $^{-2}$ s $^{-1}$ in the 2–20 keV band (e.g. Serino et al. 2014c; Negoro et al. 2016) in a scan transit. This sensitivity is sufficient to detect emission of superbursts from galactic neutron-star binaries. The typical interval of 92 min between two GSC scans is short enough not to miss bright transient events which last for several hours, such as superbursts, in almost the entire sky. Indeed, all the superbursts reported since 2009 till the time of this writing have been observed by MAXI.

In this paper we present long-lasting X-ray bursts detected with MAXI, which were observed in more than a scan transit (typically 40–50 s, Sugizaki et al. 2011). We study nine long-lasting X-ray bursts and discuss their global properties. Eight out of nine bursts have an e-folding decay time of the bolometric flux much longer than a thousand seconds, which is supposed to be the upper end of the intermediate-duration burst, whereas the decay time of the other one was about a thousand seconds. We also look into the flux levels before and after the long bursts, using the MAXI public light-curves of the sources. In section 2, we describe the sample of long X-ray bursts observed with MAXI and the method of our analysis. The results are presented in section 3. In section 4, we discuss the properties of individual events and their canonical characteristics, and then summarize our results.

2 Observations

2.1 Sample in this paper

MAXI has observed more than a hundred X-ray bursts¹. Whereas some of them are found by human inspection, most of the X-ray bursts are automatically detected by the *MAXI Nova-Alert System* (Negoro et al. 2016). The system works in real time and looks through the light curves of eight types of timescale bins (from 1 sec to 4 days) at each celestial position. Among the timescale bins, 1 scan (typically 40–50 sec) bin is useful to search for long X-ray bursts. The system searches the newest time bin for a 3 sigma excess above the average flux over the previous 9 bins (Negoro et al. 2016).

If there is a known X-ray burst source within the error circle of a sky position, where an excess is found in the light curve, we regard it as an X-ray burst event. In this paper we study the bursts whose the e-folding time is longer than 100 seconds. Seven events were detected in two or more consecutive scans, where the interval between scans is 92 min, and accordingly were selected as candidate long-lasting X-ray bursts. Among them a superburst from SAX J1747.0–2853 (on 2011 February 13, or MJD 55605) was observed also by INTEGRAL (Chenevez et al. 2011).

When a burst was detected in only one MAXI/GSC scan,

¹ <http://maxi.riken.jp/alert/novae/index.html>

which lasts 40–50 s, it is unclear whether the e-folding time of the burst was longer than 100 seconds or not, based on the MAXI/GSC data alone. We in principle exclude those events from the sample in this paper (for example, a burst from 4U 1850–086 on 2011 November 9 (MJD 55874) in section 4.2.3).

Two X-ray burst events are found to have a long duration, by combining the data of the MAXI/GSC and other satellites (See the column of “inst.” in table 1). One is a long X-ray burst from 4U 1850–086 on 2014 March 10 (MJD 56726), which was observed by Swift (in’t Zand et al. 2014). For this source, the duration of the burst was too short to be observed in multiple scans of MAXI. We did detect a significant increase of the fluxes in a MAXI scan during the burst duration expected from the Swift data.

The other one is a burst from 4U 1820–30 on 2010 March 17 (MJD 55272). MAXI failed to detect the excess of the flux in multiple scans but only in one. We nevertheless include it in our sample, because the duration of the burst was at least 75 min, as reported by in’t Zand et al. (2011), whose estimation was based on both the flux of MAXI and the flux enhancement with the RXTE/ASM.

The burst observed on 2011 October 24 was from the direction toward the globular cluster Terzan 5. Although MAXI cannot resolve the sources in a globular cluster, we identified it as a burst from EXO 1745–248, because the burst was followed by an outburst and the position of the outburst source was determined precisely by Swift XRT and Chandra (Mihara et al. 2011a; Serino et al. 2012, and references there in). Table 1 lists all the nine events.

2.2 Data in this paper

We use two types of data in the analyses. One is X-ray event data of MAXI GSC, which is used for the spectral and time-series analyses within each scan. The other is the MAXI public light-curves,² in which two separate time-resolutions (one orbit and one day) are available for each object. Figure 1 shows the orbital light curves of our sample in the 2–4 and 4–10 keV bands.³ In general, the peaks of the bursts are more prominent in 4–10 keV than in 2–4 keV bands and have a shorter decay time in the higher energy band. For the study of persistent fluxes (section 3.5), we rebin the one-day light curves into ten-day bins in order to study the persistent emissions of low flux level. The results are shown in table 2.

² <http://maxi.riken.jp/top/>

³ The public light curve of 4U 0614+091 is not available around the burst time, because a structure of the International Space Station came close to the position of the source.

2.3 Observations of normal bursts

In later sections we compare the fluxes of superbursts and normal bursts. Table 2 lists the peak bolometric flux of the normal bursts in the column F_b . In the table, we mainly refer to the previous works with various satellites. The exception is 4U 1850–086, where we use the flux of a normal X-ray burst observed with MAXI on 2010 November 2 (MJD 55502) because the previous observation with RXTE detected no X-ray burst from the source (Galloway et al. 2008). The peak photon flux of the burst was 5.8 ± 0.9 photons $\text{cm}^{-2} \text{s}^{-1}$. Assuming a black-body spectrum with the temperature of 2.0 keV, the peak bolometric flux of the burst is calculated to be $5.9 \pm 0.9 \times 10^{-8}$ erg $\text{cm}^{-2} \text{s}^{-1}$. This peak flux with MAXI agreed with those of 28 normal bursts from this source in 2002, observed with HETE-2/WXM (Ricker et al. 2003; Shirasaki et al. 2003; Suzuki et al. 2006). Thus, the flux of the bursts has not changed much between 2002 and 2010.

3 Data analysis and Results

3.1 Variability within the scans of maximum fluxes

A brief brightening with a time scale of a normal X-ray burst has been commonly observed immediately before, or at the onset of, a superburst, and is referred to as “precursor” (Strohmayer & Brown 2002; Kuulkers et al. 2002; Strohmayer & Markwardt 2002; in’t Zand et al. 2004). In figure 2 we plotted the light curves of the bursts, correcting for the effective area, at the brightest scans in the 2–20 keV energy band with 1 s time resolution to search for potential precursors. The light curve of the first burst from 4U 1850–086 (on 2014 March 10, or MJD 56726) is not shown here, because the observed flux was too low to extract a meaningful light curve with the photons observed in a scan (see figure 1).

The light curves of some sources are contaminated with an emission from nearby bright sources. That of EXO 1745–248 is the worst; the entire period is contaminated with an emission from GX 3+1 and GX 5–1. Hence, it is dropped from figure 2. The light curves of SLX 1735–269 and SAX J1747.0–2853 are partially affected with contaminating sources. The affected time intervals are indicated with shaded regions in figure 2.

We find no obvious burst-like variability (figure 2). The light curve of 4U 0614+091 shows a hint of possible variation, and those of relatively short bursts from 4U 1820–30 and 4U 1850–086 show a trend of decay. All the other light curves are consistent with a constant flux.

3.2 Spectral analyses

We perform spectral analysis of the bursts, using XSPEC, to study a potential spectral evolution during a burst. The spectrum of each scan is fitted with a model, unless the statistics

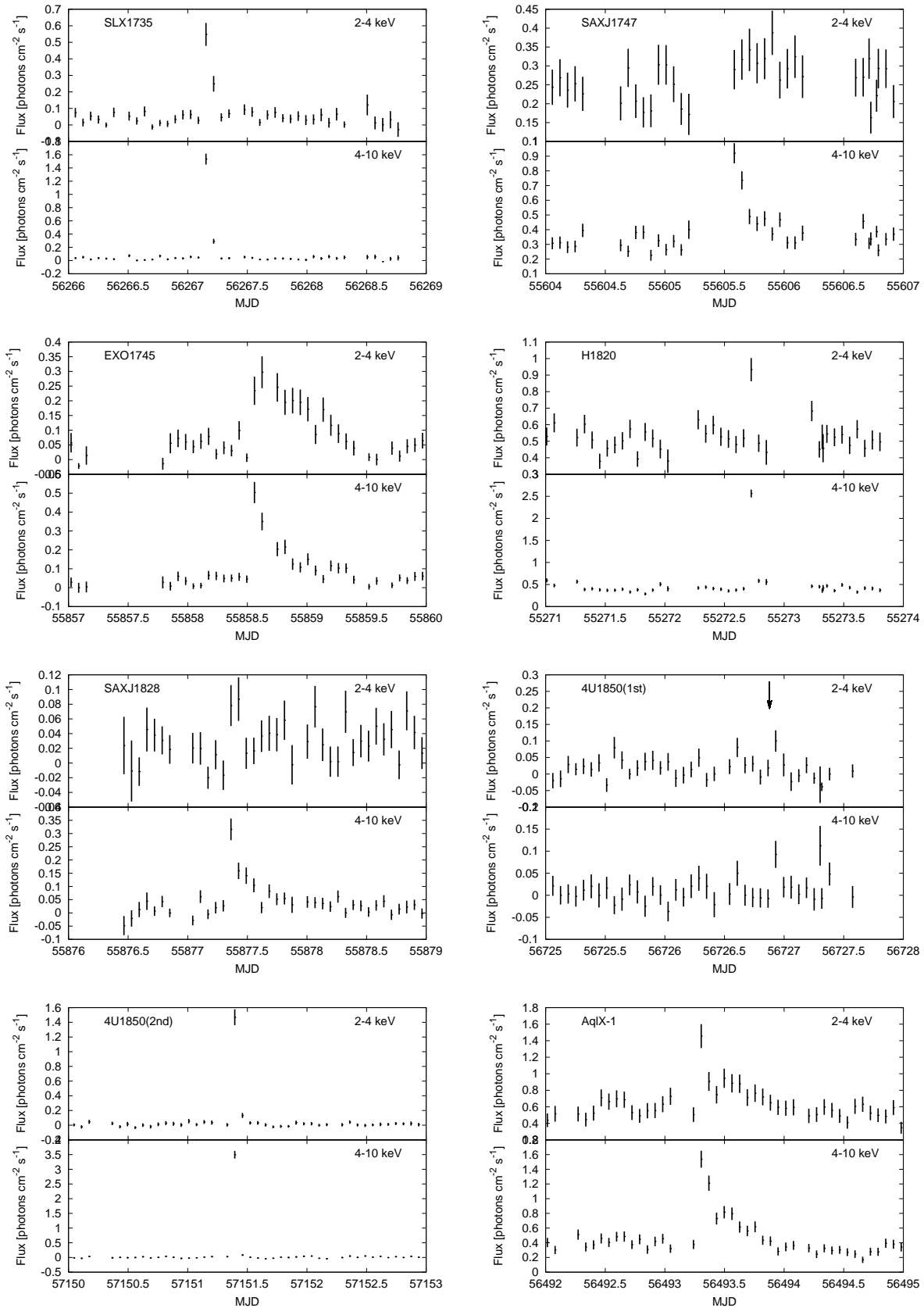


Fig. 1. The light curves of the bursts in the 2–4 and 4–10 keV bands. Each data point corresponds to a scan. The typical time interval between two scans is 92 min. For the first event from 4U 1850–086, the time of the Swift detection is indicated with an arrow. The light curve of 4U 0614+091 is not available around the burst time, because a structure of the International Space Station came close to the position of the source.

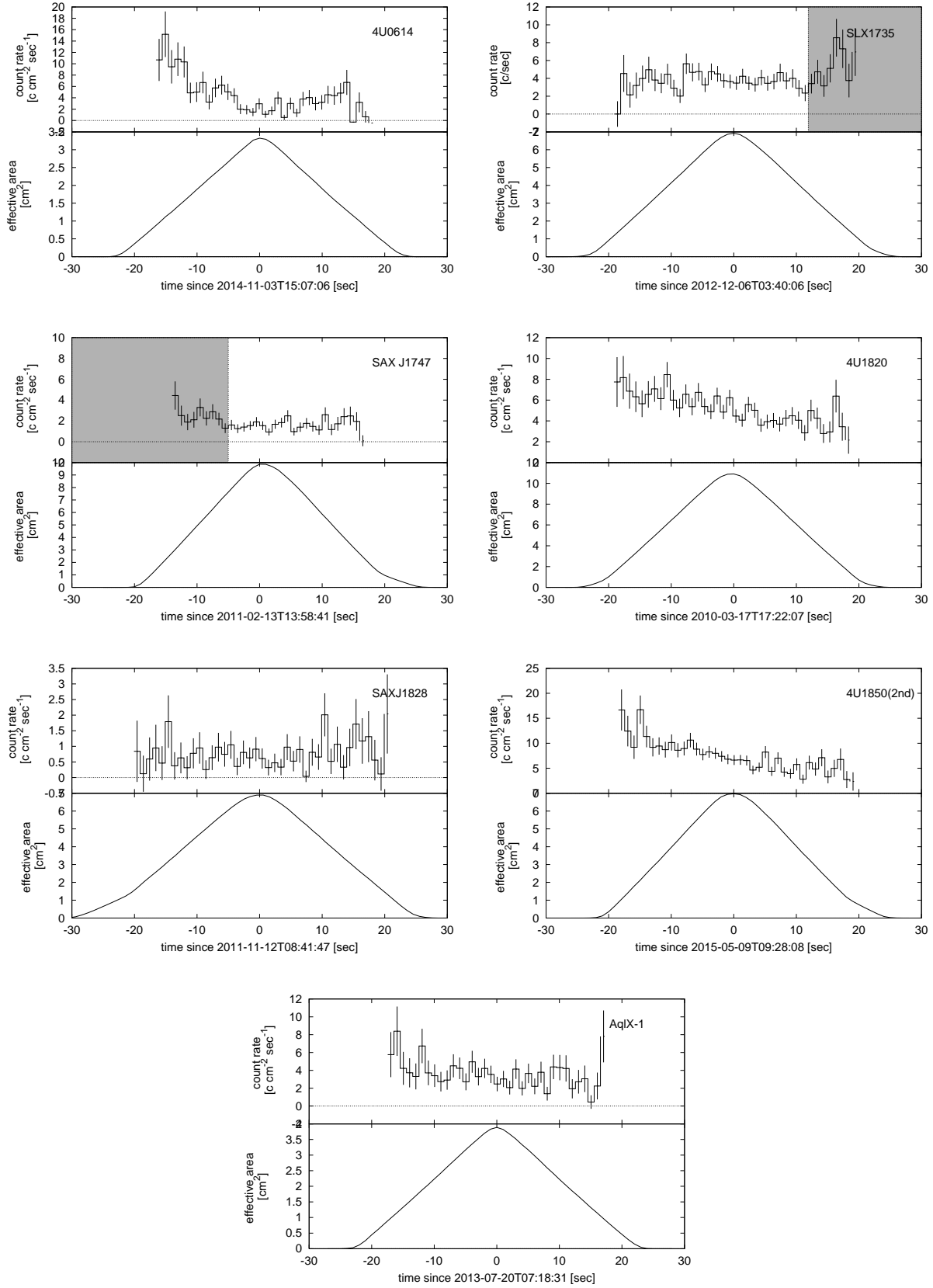


Fig. 2. The light curves of the brightest scans of each burst in the 2–20 keV energy band with 1 s time resolution. The light curves are corrected for the effective area, whose time variation is displayed in the bottom panel of each burst. The shaded regions represent the time intervals affected by contamination sources. The light curve of the first burst from 4U 1850–086 (on 2014 March 10, or MJD 56726) is not shown here, because the observed flux was too low to extract a meaningful light curve with the photons observed in a scan.

of the data is too poor, in which case the spectra are summed for multiple scans before fitted (the rows in table 3, in which the column MJD has a range, indicate the cases of spectra with multiple scans combined).

We adopt the blackbody model (Bbody in XSPEC), which is characterized with a blackbody temperature and bolometric flux, for the burst component. The persistent emission from the sources may also have to be considered. For three weak sources (EXO 1745–248, SAX J1828.5–1037, and 4U 1850–086), the contribution of their persistent-emission component is negligible. However, the other sources (4U 0614+091, SLX 1735–269 SAX J1747.0–2853, 4U 1820–30, and Aql X-1) had a significant persistent emission, which is incorporated in the model-fitting. We model the persistent emission with a power law (Powerlaw) or a power law with high-energy exponential-cutoff model (Cutoffpl), and assume that the persistent emission did not change during and shortly before the burst. Thus we used a combined spectrum from scans immediately before the burst to represent the persistent-emission spectrum.

The spectral parameters of the persistent-emission component of each spectrum during a burst should have common value. A simple way to fulfill the requirement is using the fixed model parameters which are derived by a fit of the persistent spectrum. However, this method has a problem that the errors on the parameters of the persistent-emission component are not considered correctly at the fit of the burst spectra.

Then we adopted a joint fit method. We jointly fitted all the spectra before and during the burst for multiple scans, if available. We linked the spectral parameters of the persistent-emission component, whereas the temperature and normalization of the blackbody component for each spectrum were allowed to vary. The normalization of blackbody of the persistent spectrum was fixed to zero. For example, the burst from SLX 1735–269 on 2012 December 6 (MJD 56267) was detected for two scans, and thus we had three spectra in total; two spectra during the burst and one spectrum of the persistent emission before the burst. We jointly fitted these three spectra at a time, where the spectral parameters of the persistent-emission component were common to all three spectra.

The column densities of the absorption are included for the two sources only that have a significant absorption: SAX J1747.0–2853 with $\sim 10 \times 10^{22} \text{ cm}^{-1}$ (Natalucci et al. 2004) and SAX J1828.5–1037 with $4.1 \times 10^{22} \text{ cm}^{-1}$ (Degenaar & Wijnands 2008). We used Wabs model to incorporate the column densities as a fixed parameter in the model fitting.

Table 3 summarizes the result of the spectral fittings. We find that the observed peak temperatures were typical of X-ray bursts. All the sample events showed cooling, which were particularly prominent in the early phases. This cooling is consistent with the difference in the light-curves in the two different energy-bands; the flux in the 4–10 keV band decayed faster than

that in the 2–4 keV band in most bursts (figure 1). This is the evidence that the phenomenon is not an accretion event but a thermonuclear burst.

3.3 Calculation of burst parameters

In table 4, we list the parameters of the bursts. F_{obs} is the bolometric flux at the observed peak time derived with spectral fitting (section 3.2). F_{max} , τ_{LB} , d , and E_{b} are the possible maximum bolometric flux, the e-folding time, the distance to the source, and the total energy of the burst, respectively.

For the first burst (on 2014 March 10, or MJD 56726) of 4U 1850–086, F_{obs} in the table is taken simply from in’t Zand et al. (2011). Similarly, τ_{LB} of 4U 1820–30 and 4U 1850–086 (first) in table 4 are taken from in’t Zand et al. (2011) and in’t Zand et al. (2014), respectively.

For the other sources, we fit the light curves of the bolometric fluxes (table 3) with a simple exponential function and estimate τ_{LB} . Then we estimate the possible maximum bolometric flux F_{max} by extrapolating the exponential function to the epoch of the previous scan transit.

For SAX J1747.0–2853, we calculate F_{max} , using the peak time observed by INTEGRAL (Chenevez et al. 2011) instead of the time of the previous scan transit. The calculated F_{max} is $1.9 \times 10^{-8} \text{ ergs cm}^{-2} \text{ s}^{-1}$. Chenevez et al. (2011) reported the peak flux as $6.7 \times 10^{-8} \text{ ergs cm}^{-2} \text{ s}^{-1}$ in 3–30 keV (including persistent flux). Using the temperature at the peak and assuming that the persistent component was not changed, we calculate the bolometric flux at the peak to be $6.9 \times 10^{-8} \text{ ergs cm}^{-2} \text{ s}^{-1}$. This peak flux is higher than the peak flux estimated from MAXI data. The fact indicates that the initial decay was much faster than the decay in late time or that there was a normal X-ray burst at the beginning of the superburst.

The burst energy E_{b} is calculated, using F_{obs} , τ_{LB} and d . Note that these E_{b} are the lower limits of the true energy, because the true peak fluxes of the bursts would be larger than the observed values, if the peak-flux time had been out of the observed window; in that case, the burst energy could be as large as $E_{\text{b}}(F_{\text{max}}/F_{\text{obs}})$. The derived burst energies E_{b} are distributed around 10^{41} – 10^{42} erg, which is comparable with a typical energy of intermediate-duration bursts (10^{41} erg, Falanga et al. 2008) and superbursts (10^{42} erg, Kuulkers 2004).

The shortest e-folding time in our sample is ~ 0.27 hours from 4U 1850–086 (on 2014 March 10, or MJD 56726), and the longest one is 5.2 hours from 4U 0614+091 (on 2014 November 3, or MJD 56964). We then compare the e-folding times of our sample with the previous ones, if any, in literature. The previous superburst from 4U 0614+091 (on 2005 March 12, or MJD 53441) was reported by Kuulkers et al. (2010) and the e-folding time was 2.1 hours. The one from 4U 1820–30 (on 1999 September 9, or MJD 51430) (Strohmayer & Brown

2002) had an e-folding time of ~ 1 hour. The e-folding time of the event from 4U 1820–30 in our sample (table 4) may appear to be shorter than that by a factor of two. However, the superburst that the MAXI/GSC detected could well have started roughly 0.5 hr before the scan, and in that case the light-curves of both the superbursts would be consistent with each other, as pointed out by in’t Zand et al. (2011).

There are two bursts from 4U1850–086 in our sample and the e-folding times of the first (on 2014 March 10, or MJD 56726) and second (on 2015 May 9, or MJD 57151) bursts were 0.27 and 0.71 hours, respectively. A large variation in the decay time of superbursts from the same source has been known for at least three superburst sources: 4U 1636–53 (Wijnands 2001), GX 17+2 (in’t Zand et al. 2004), and Ser X-1 (Cornelisse et al. 2002a; Kuulkers 2009). Our discovery has added another example to confirm the large variation in the decay time in long-lasting X-ray bursts. We discuss the classification of the sample events by the duration in section 4.1.

3.4 First type-I bursts after the long bursts

Burst quenching is a common phenomenon after a superburst (Cornelisse et al. 2000; Kuulkers et al. 2002). Table 4 lists the time of the first X-ray bursts after the long bursts that we detected.

Linares et al. (2011) reported that a normal X-ray burst from SAX J1747.0–2853 (on 2011 February 13, or MJD 55605) was observed 25 days after the superburst. Normal X-ray bursts from 4U 1820–30 and Aql X-1 were observed by MAXI 1549 and 389 days after the long bursts, respectively. The first X-ray burst from 4U 1850–086 after the long burst on 2014 March 10 (MJD 56726) was observed on 2015 May 9 (MJD 57151, 425 days after the long burst), which is the second event in our sample. After the second event, another X-ray burst with a longer duration than the scan transit (~ 40 sec) on 2015 November 11 (MJD 57337) occurred from the same source (see section 4.2.3). Thus, the quenching time of the second event was 186 days. No X-ray burst was detected by MAXI after the long bursts for the other sources (4U 0614+091, SLX 1735–269, EXO 1745–248, and SAX J1828.5–1037).

3.5 Persistent emissions of the sources

MAXI can monitor the persistent fluxes of the burst sources, and therefore MAXI is an optimum instrument for studying the relation between the persistent emissions and superbursts and the potential change of the persistent flux after a superburst. Using the MAXI light curves of one-day bin in the public data archive, we calculate ten-day average fluxes in the 2–20 keV band (10 days – 1 day) before and (1 day – 10 days) after each burst.⁴ The

⁴ For 4U 0614+091, we use the data of 30–25 days and 1 day before, and 2–10 days after the burst, because the public light curve of 4U 0614+091

photon count rates are converted to the energy fluxes, assuming the crab-like spectrum. The results are given in the columns F_{before} and F_{after} in table 2.

We find some significant changes in the flux after the bursts for some sources. In order to compare the changes of the persistent fluxes after the bursts with the intrinsic variations, we plotted in figure 3 the distribution of the ten-day average fluxes of each source in the same energy band, using all the available MAXI data.

An increase in the persistent flux is apparent in EXO 1745–248, and is marginally confirmed in SAX J1828.5–1037, 4U 0614+091, and the first sample of 4U 1850–086 (on 2014 March 10, or MJD 56726). The burst from Aql X-1 occurred during the decay part of an outburst while the persistent emission was continuously decreasing. Therefore, the persistent flux after the superburst is expected to be significantly lower than that before the burst.

4 Discussion and conclusion

4.1 Discussion about overall properties

Before the MAXI era, most of the known superburst sources were persistent and bright. Kuulkers (2004) summarized the persistent luminosities of superbursters, and concluded that all of them were at or above 10% of Eddington luminosity. In contrast, Falanga et al. (2008) showed that intermediate-duration bursts could occur at $\leq 1\%$ Eddington luminosity.

Figure 4 shows the ratio γ of the persistent fluxes of each source before and after the superburst to the peak flux of the normal bursts from the same source. The peak flux of normal bursts of a burster is usually its Eddington limit or close. Accordingly, γ here is a good approximation to the Eddington ratio of the source fluxes (Lewin et al. 1993). 4U 1820–30 has the largest γ in our sample, which is consistent with that listed in Kuulkers (2004). Six of the other sources are transients (table 2). The calculated ratios of SAX J1747.0–2853 and Aql X-1 are around 0.1 and the superbursts of these sources occurred during outbursts. The ratios are $\lesssim 0.01$ for six out of nine in our MAXI sample. Among them, two sources, EXO 1745–248 and SAX J1828.5–1037, are transient and they might have been in quiescence at the time of the superbursts. The other four of the six are ultracompact X-ray binaries (UCXBs) or candidate UCXBs (in’t Zand et al. 2007), which are known to have persistent luminosity of a small Eddington ratio.

We should note that a selection bias may be significant; it is easier with MAXI to find superbursts from sources with weaker persistent emissions, because burst signals over fluctuations of the persistent component are more prominent in fainter sources than brighter ones. We need further investigations to find whether superbursts from bright sources exist in the MAXI

is not available from 24–2 days before and 1 day after the burst.

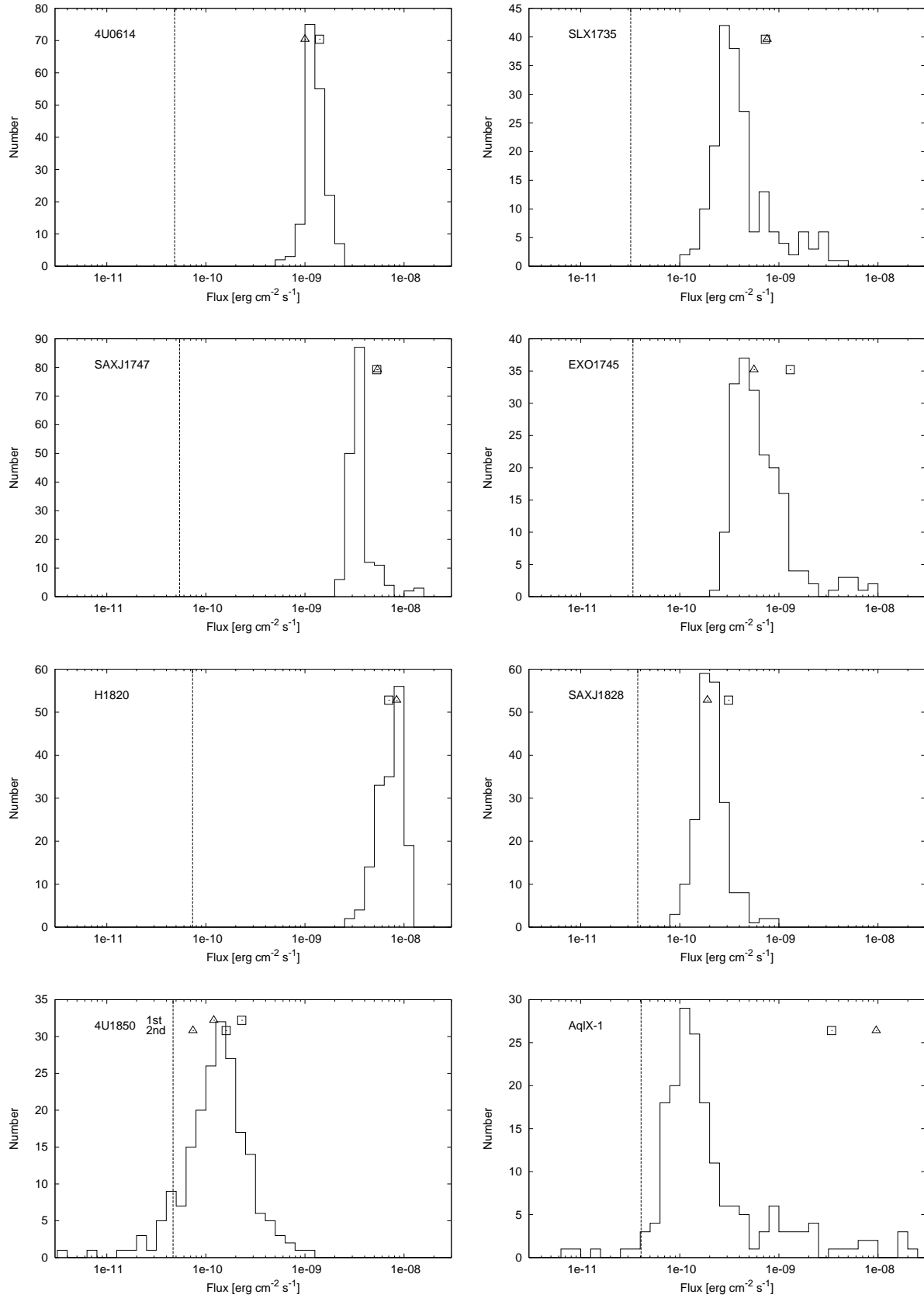


Fig. 3. The persistent fluxes of each source before (triangles) and after (squares) the bursts. The histograms are the distributions of ten-day average flux of the sources. The vertical dashed-lines indicate the typical errors on the ten-day average fluxes of the sources, which correspond to the 1 sigma detection limit for ten days.

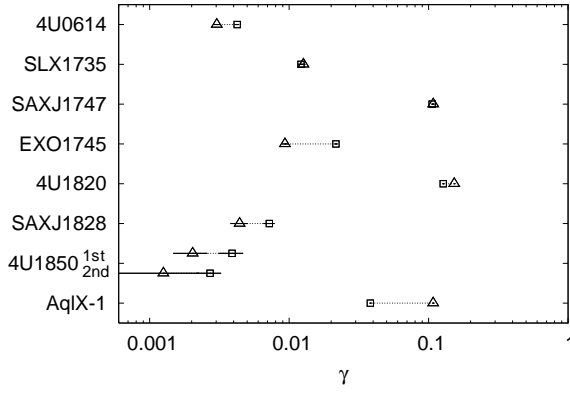


Fig. 4. The persistent fluxes before (triangles) and after (squares) the long bursts, normalized to the peak fluxes of normal bursts γ . For 4U 1850–086, there are two pairs of points, corresponding to the two bursts.

data or not.

Next, we plot in figure 5 the e-folding decay time τ_{LB} of the burst versus the normalized peak flux, which is the peak flux of our sample (F_{obs} or F_{max} in table 4) normalized to the peak flux of normal bursts (F_b in table 2). Four bursts (from SLX 1735–269, 4U 1820–30, and two bursts from 4U 1850–086) showed an e-folding decay time τ_{LB} shorter than one hour and had a relatively high peak flux. 4U 0614+091, SLX 1735–269, 4U 1820–30 and 4U 1850–086 are (or are suppose to be) UCXBs, from which intermediate-duration bursts are often observed. The observed durations and fluxes of the bursts from these sources except 4U 0614+091 are consistent with intermediate-duration bursts. Therefore, we argue that the four long bursts with an e-folding decay time τ_{LB} shorter than one hour which MAXI detected from SLX 1735-269, 4U 1820-30 and 4U 1850-086 should be classified as intermediate bursts. Notably, the burst from SLX 1735-269 is the longest intermediate burst ever found. Consequently, the other five events are superbursts.

The derived peak fluxes have a large ambiguity due to the unknown delay from the peak time of the burst to the scan time. Nevertheless, the peak flux and τ_{LB} seem to show a significant anti-correlation. In other words, brighter bursts decay faster. Consequently, the total emitting energy of the bursts clusters around 10^{41} – 10^{42} erg. Given that the data contain two classes of intermediate-duration burst and superburst, it appears that bursts with a wide range of durations follow the same relation. The suggested anti-correlation between the peak flux and the e-folding time does not hold for normal bursts, because the normalized peak fluxes of normal bursts are by definition equal to, or smaller than, unity, whereas the durations of normal bursts are more than an order of magnitude shorter than an hour.

We calculate the parameters of nuclear reactions, using the cooling model given by Cumming & Macbeth (2004). The

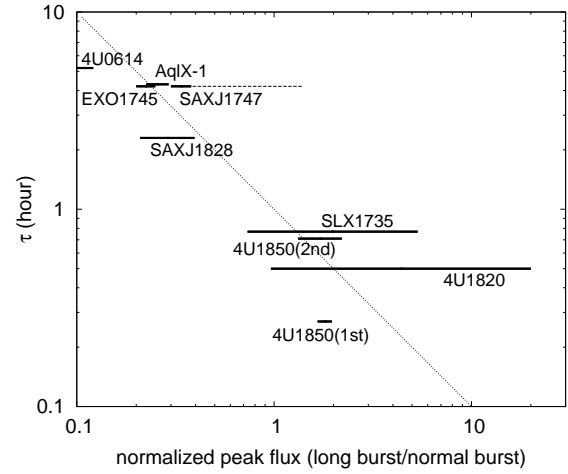


Fig. 5. A scatter plot of the fluxes of the long bursts normalized to those of normal bursts and τ_{LB} of the long bursts. The lower ends of the fluxes are the observed ones (F_{obs}), and the upper ends are possible maximum fluxes (F_{max}). For the first event of 4U 1850–086, we simply plot the error of the observed flux. The dashed line of the SAX J1747.0–2853 shows F_{max} observed by INTEGRAL. The relation [normalized flux = $1/\tau$] is shown with a dotted line.

model parameters are the ignition column depth y_{12} in units of 10^{12} g cm $^{-2}$ and energy release per unit mass E_{17} in units of 10^{17} erg g $^{-1}$. The model approximates the light curves of the bursts with a broken power-law function, which has the decay indices of -0.2 and $-4/3$ in the early and late phases, respectively. The parameter t_{cool} , indicating the transition time between the two indices, is proportional to $y_{12}^{3/4}$. Therefore, a burst with a larger ignition column depth y_{12} stays bright for a longer period. The luminosity L of a burst is a direct function of the energy release E_{17} : $L \propto E_{17}^{7/4}$ and $L \propto E_{17}^{1/2}$ in the early and late phases, respectively. Thus, we can obtain these parameters by fitting the light curves of the bursts.

This analysis requires good statistics. Hence, we used the events with more than two observed scans only: 4U 0614+091, SAX J1747.0–2853, EXO 1745–248, SAX J1828.5–1037, and Aql X-1. For EXO 1745–248, we considered the cases of two possible distances. The uncertainties of the burst peak time (and the flux at that time) are the major cause of the systematic error, because the peak-flux time may be out of the observed window as discussed in section 3.3. Note that the maximum values of the peak fluxes are listed in the column F_{max} in table 4 and the minimum values are equal to F_{obs} in the table.

We perform calculation of the model parameters for seven possible peak times for a burst with model fitting, except for SAX J1747.0–2853, where we simply accept the burst peak-time observed with INTEGRAL. Figure 6 shows the results. Compared with the works in literature for the past superbursts (for example, Cumming et al. 2006; Keek et al. 2008), our results are in the typical range of the parameters.

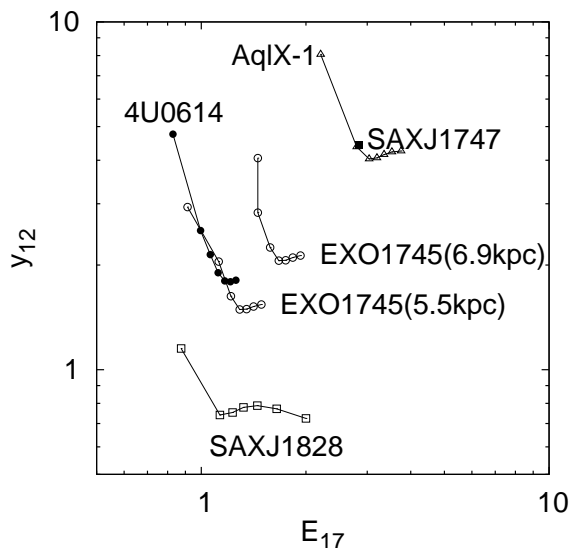


Fig. 6. A scatter plot of the released energy E_{17} (10^{17} erg g^{-1}) and the ignition column depth y_{12} (10^{12} g cm^{-2}). Each of seven points per event, connected with a line, corresponds to the result of fitting with a different assumed peak time, δt days before the first observation ($\delta t = 0.001, 0.01, 0.02, 0.03, 0.04, 0.05$, or 0.06). The results of the same source are plotted with the same symbol and are connected with a solid line. For EXO 1745–248, two different cases for different distances are plotted. In the case of the burst from SAX J1747.0–2853, the burst peak was observed by INTEGRAL, and hence we use the time of it (a single point in the figure).

Burst quenching has been studied systematically by Cumming & Macbeth (2004) and Keek et al. (2012). There is only an event with a short (<100 days) quenching time in our sample (table 4). A normal X-ray burst from SAX J1747.0–2853 was observed 25 days after the superburst (Linares et al. 2011). The model by Cumming & Macbeth (2004) gives an estimation of the quenching time. Using y_{12} , E_{17} (figure 6) and γ (figure 4), we calculated the quenching time to be 26 days, which is consistent with the observed one. Good agreement between the predicted and the observed values of quenching time have been reported for superbursts (for example from 4U 1636–536 on 1999 June 26 (MJD 51324) Kuulkers et al. 2004; from GX 17+2 on 1996 September 14 (MJD 50340) and on 1999 October 1 (MJD 51452) in’t Zand et al. 2004; from 4U 0614+091 on 2005 March 12 (MJD 53441) Kuulkers et al. 2010). Our result adds another example to that, and confirms the relation.

4.2 Discussion on individual sources

4.2.1 4U 0614+091

A superburst from 4U 0614+091 was observed on 2005 March 12 (MJD 53441) with RXTE/ASM before the MAXI era. Kuulkers et al. (2010) reported that the source had experienced brightening in the hard X-ray (15–50 keV) data be-

fore the superburst. Then, we look through the light curve of Swift/BAT transient monitor results provided by the Swift/BAT team (Krimm et al. 2013), and find that the superburst observed by MAXI also occurred at the time of the high persistent flux. These facts suggest that some special accretion condition may induce superbursts.

Kuulkers et al. (2010) pointed out that this source showed flaring and quiet periods in the persistent emission. They found that an intermediate-duration burst occurred during the calm period and that all the other bursts including the superburst occurred during the flaring period. We have found the same trend in the MAXI data; the superburst observed by MAXI also occurred during the flaring period.

4.2.2 Low accretion rate in EXO 1745–248 and SAX J1828.5–1037 before the superbursts

We find that EXO 1745–248 and SAX J1828.5–1037 had a very weak persistent emission before the superbursts. It is unclear how these superbursts were ignited during the periods of low accretion rate. Indeed, Altamirano et al. (2012) has argued that the low accretion rate of EXO 1745–248 before the superburst makes the ignition difficult. Another case of a superburst during the period of low accretion was from so-called “burst-only source”, SAX J1828.5–1037 (Cornelisse et al. 2002c; Cornelisse et al. 2002b). Campana (2009) estimated the 0.5–10 keV unabsorbed flux in quiescence to be 1.5×10^{-13} erg cm^{-2} s^{-1} . Hands et al. (2004) reported that the source had been observed 2001 March and 2002 September, but had not been detected in the latter observation with the upper limit of the flux of 2×10^{-14} erg cm^{-2} s^{-1} in the 2–10 keV band.

At least two outbursts have been observed from SAX J1828.5–1037 so far, in 2001 (Hands et al. 2004) and in 2008 (Degenaar & Wijnands 2008). The flux level during the latter outburst was at about 10^{-12} erg cm^{-2} s^{-1} . The distribution of 10-day average fluxes of this source observed in 2011 by MAXI/GSC (figure 3) clusters around 10^{-10} erg cm^{-2} s^{-1} , and the fluxes are higher than those of above-mentioned outburst. Note that the observed flux in figure 3 is higher than the real one due to the contamination of the Galactic ridge emission. MAXI can not detect an outburst with the flux of 10^{-12} erg cm^{-2} s^{-1} . On the other hand, the peak flux of normal X-ray burst from this source was $4.3 \pm 1.6 \times 10^{-8}$ erg cm^{-2} s^{-1} (table 2). An outburst with the flux larger than 1/100 of that at the peak of an X-ray burst should be detected by MAXI/GSC, if it occurs.

In both the cases of EXO 1745–248 and SAX J1828.5–1037, an increase of the persistent flux was observed (figure 3). Serino et al. (2012) has shown that the superburst of EXO 1745–248 was followed by a short outburst for about five days in the light curve EXO 1745–248. They

discussed the possibilities that the outburst was induced by the superburst. The increase of the persistent flux of SAX J1828.5–1037 may be another example of an outburst following a superburst.

4.2.3 Correlation between accretion rate and burst type in 4U 1850–086

Although RXTE observed 1187 X-ray bursts in more than 10 years of observations, none was observed from 4U 1850–086 (Galloway et al. 2008). In contrast, HETE-2 observed 28 normal bursts from 4U 1850–086 in 2002 (Suzuki et al. 2006). In general, the activities of normal X-ray bursts are thought to be related to the persistent luminosities. Then, we plot the persistent flux observed by RXTE/ASM⁵ or MAXI and the time of normal bursts in figure 7. The source was in the HETE-2/WXM field of view (FoV) in May–September from 2001 to 2005, because HETE-2 pointed toward the anti-solar direction. The periods when the source was in the HETE-2 FoV are indicated in figure 7.

MAXI observed one normal burst and four long bursts from this source. Two of the long bursts are listed in table 4. The durations of the others (on 2011 November 9, MJD 55874 and on 2015 November 11, MJD 57337) were longer than those of the scans (75 s and 40 s, respectively). However, the flux dropped back to the background level in the next scan. Therefore, the durations of these bursts are unclear, and we have excluded them from the sample in this paper.

Figure 7 shows a possible correlation between the accretion rate and the burst type. All the normal bursts were observed when the persistent flux was relatively high, whereas the long bursts occurred when the persistent flux was low. The average persistent flux observed by ASM for 28 normal X-ray bursts was 50 mCrab with the standard deviation of 25 mCrab. The source was not significantly detected just before the four long bursts and 1-sigma flux upper-limits in these observations were about 5 mCrab. A trend that the burst type changes in the phase of low persistent flux has been reported for intermediate-duration bursts from 4U 0614+091 (Kuulkers et al. 2010, and references therein). Our result is the first indication that the trend may extend to long X-ray bursts from 4U 1850–086, although the statistics of the sample is still limited to derive definite conclusion.

4.3 Conclusions

We studied the properties of nine long X-ray bursts from eight sources observed with MAXI in 2009–2015. We found that six out of the eight sources were transient and five out of the nine bursts occurred when the persistent luminosities were lower

than 1% of the Eddington luminosity. These trends are contrastive to the superbursts observed before the MAXI era, which originated from bright persistent sources. There is a negative correlation between the durations and the peak fluxes of our sample. The total released energy of them clusters between 10^{41} – 10^{42} erg. Using the light curves with RXTE/ASM and MAXI, we compared the flux levels of persistent emissions at the time of “normal” and long bursts from 4U 1850–086. We found that the four long bursts occurred in the phase of relatively low persistent flux, whereas normal X-ray bursts occurred during outbursts.

Acknowledgments

This research has made use of the MAXI data provided by RIKEN, JAXA and the MAXI team. This research was supported by JSPS KAKENHI Grant Number 24740186, JP16K17717.

References

- Altamirano, D., Keek, L., Cumming, A., et al. 2012, MNRAS, 426, 927
- Asada, M., Negoro, H., Sugizaki, M., et al. 2011, The Astronomer’s Telegram, 3760, 1
- Brandt, S., Castro-Tirado, A. J., Lund, N., et al. 1992, A&A, 262, L15
- Campana, S. 2009, ApJ, 699, 1144
- Chenevez, J., Brandt, S., Kuulkers, E., et al. 2011, The Astronomer’s Telegram, 3183, 1
- Cornelisse, R., Heise, J., Kuulkers, E., Verbunt, F., & in’t Zand, J. J. M. 2000, A&A, 357, L21
- Cornelisse, R., Kuulkers, E., in’t Zand, J. J. M., Verbunt, F., & Heise, J. 2002a, A&A, 382, 174
- Cornelisse, R., Verbunt, F., in’t Zand, J. J. M., Kuulkers, E., & Heise, J. 2002b, A&A, 392, 931
- Cornelisse, R., Verbunt, F., in’t Zand, J. J. M., et al. 2002c, A&A, 392, 885
- Cumming, A. & Bildsten, L. 2001, ApJL, 559, L127
- Cumming, A. & Macbeth, J. 2004, ApJL, 603, L37
- Cumming, A., Macbeth, J., in’t Zand, J. J. M., & Page, D. 2006, ApJ, 646, 429
- Degenaar, N. & Wijnands, R. 2008, The Astronomer’s Telegram, 1831, 1
- Falanga, M., Chenevez, J., Cumming, A., et al. 2008, A&A, 484, 43
- Fujimoto, M. Y., Hanawa, T., & Miyaji, S. 1981, ApJ, 247, 267
- Galloway, D. K., Muno, M. P., Hartman, J. M., Psaltis, D., & Chakrabarty, D. 2008, ApJS, 179, 360
- Hands, A. D. P., Warwick, R. S., Watson, M. G., & Helfand, D. J. 2004, MNRAS, 351, 31
- Harris, W. E. 2010, ArXiv e-prints
- in’t Zand, J., Linares, M., & Markwardt, C. 2014, The Astronomer’s Telegram, 5972, 1
- in’t Zand, J., Serino, M., Kawai, N., & Heinke, C. 2011, The Astronomer’s Telegram, 3625, 1
- in’t Zand, J. J. M., Cornelisse, R., & Cumming, A. 2004, A&A, 426, 257
- in’t Zand, J. J. M., Cumming, A., van der Sluys, M. V., Verbunt, F., & Pols, O. R. 2005, A&A, 441, 675
- in’t Zand, J. J. M., Jonker, P. G., & Markwardt, C. B. 2007, A&A, 465, 953

⁵ quick-look results provided by the ASM/RXTE team: http://xte.mit.edu/ASM_lc.html

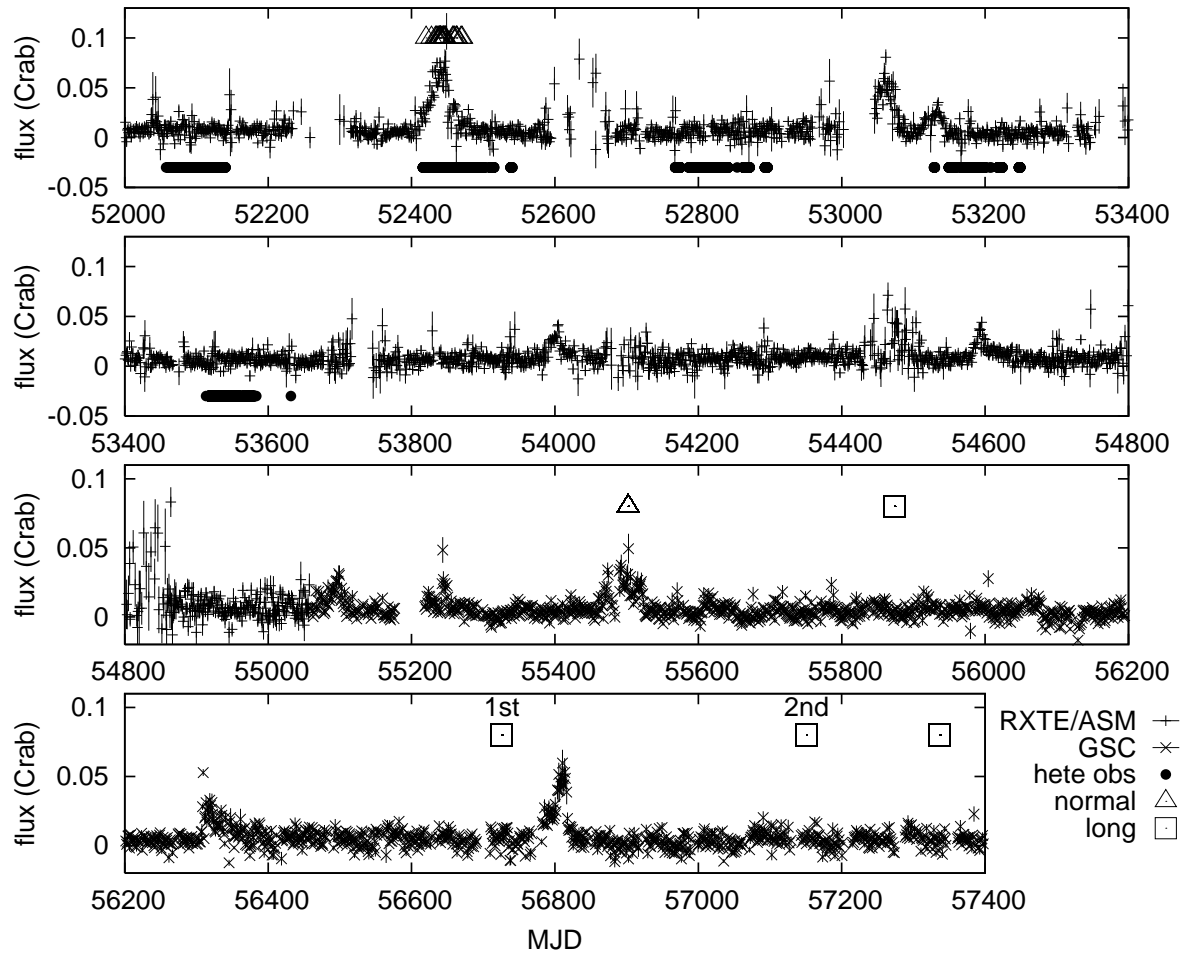


Fig. 7. The persistent fluxes of 4U 1850–086 and the epochs of bursts. The persistent fluxes observed by RXTE/ASM (plus) and MAXI/GSC (cross) are plotted. The circles show the periods when the source was in the HETE-2/WXM FoV. The triangles and squares show the time of normal and long bursts, respectively.

Keek, L., Heger, A., & in't Zand, J. J. M. 2012, *ApJ*, 752, 150
 Keek, L., in't Zand, J. J. M., Kuulkers, E., et al. 2008, *A&A*, 479, 177
 Krimm, H. A., Holland, S. T., Corbet, R. H. D., et al. 2013, *ApJS*, 209, 14
 Kuulkers, E. 2004, *Nuclear Physics B Proceedings Supplements*, 132, 466
 Kuulkers, E. 2009, *The Astronomer's Telegram*, 2140, 1
 Kuulkers, E., in't Zand, J., Homan, J., et al. 2004, in *American Institute of Physics Conference Series*, Vol. 714, *X-ray Timing 2003: Rossi and Beyond*, ed. P. Kaaret, F. K. Lamb, & J. H. Swank, 257–260
 Kuulkers, E., in't Zand, J. J. M., Atteia, J.-L., et al. 2010, *A&A*, 514, A65
 Kuulkers, E., in't Zand, J. J. M., van Kerkwijk, M. H., et al. 2002, *A&A*, 382, 503
 Lewin, W. H. G., van Paradijs, J., & Taam, R. E. 1993, *Space Sci. Rev.*, 62, 223
 Linares, M., Altamirano, D., Watts, A., et al. 2011, *The Astronomer's Telegram*, 3217
 Matsuoka, M., Kawasaki, K., Ueno, S., et al. 2009, *PASJ*, 61, 999
 Mihara, T., Matsuoka, M., Sugizaki, M., et al. 2011a, *The Astronomer's Telegram*, 3729
 Mihara, T., Nakajima, M., Sugizaki, M., et al. 2011b, *PASJ*, 63, 623
 Natalucci, L., Bazzano, A., Cocchi, M., et al. 2004, *A&A*, 416, 699

Natalucci, L., Bazzano, A., Cocchi, M., et al. 2000, *ApJL*, 543, L73
 Negoro, H., Asada, M., Serino, M., et al. 2012, *The Astronomer's Telegram*, 4622, 1
 Negoro, H., Kohama, M., Serino, M., et al. 2016, *PASJ*, 68, S1
 Negoro, H., Suzuki, K., Masumitsu, T., et al. 2015, *The Astronomer's Telegram*, 7500
 Ortolani, S., Barbuy, B., Bica, E., Zoccali, M., & Renzini, A. 2007, *A&A*, 470, 1043
 Ricker, G. R., Atteia, J.-L., Crew, G. B., et al. 2003, in *American Institute of Physics Conference Series*, Vol. 662, *Gamma-Ray Burst and Afterglow Astronomy 2001: A Workshop Celebrating the First Year of the HETE Mission*, ed. G. R. Ricker & R. K. Vanderspek, 3–16
 Serino, M., Matsuoka, M., Ueno, S., et al. 2014a, *The Astronomer's Telegram*, 5978
 Serino, M., Mihara, T., Matsuoka, M., et al. 2012, *PASJ*, 64, 91
 Serino, M., Nakahira, S., Mihara, T., et al. 2014b, *The Astronomer's Telegram*, 6668, 1
 Serino, M., Sakamoto, T., Kawai, N., et al. 2014c, *PASJ*, 66, 87

Table 1. The list of the bursts studied in this paper.

Name	date	MJD	inst.	ref.
4U 0614+091	2014-11-03	56964		A
SLX 1735–269	2012-12-06	56267		B
SAX J1747.0–2853	2011-02-13	55605	INTEGRAL	C
EXO 1745–248	2011-10-24	55858		D, E, F
4U 1820–30	2010-03-17	55272	RXTE	G
SAX J1828.5–1037	2011-11-12	55877		H
4U 1850–086 (1st)	2014-03-10	56726	Swift	I, J
(2nd)	2015-05-09	57151		K
Aql X-1	2013-07-20	56493		—

References are (A) Serino et al. 2014b, (B) Negoro et al. 2012, (C) Chenevez et al. 2011, (D) Mihara et al. 2011a, (E) Serino et al. 2012, (F) Altamirano et al. 2012, (G) in't Zand et al. 2011, (H) Asada et al. 2011, (I) in't Zand et al. 2014, (J) Serino et al. 2014a, (K) Negoro et al. 2015.

Table 2. The properties of the persistent emissions and normal bursts of the bursters.

Name	transient	F_b^* (10^{-8} ergs cm $^{-2}$ s $^{-1}$)	$F_{\text{before}}^\dagger$ (10^{-11} ergs cm $^{-2}$ s $^{-1}$)	F_{after}^\dagger	ref. ‡
4U 0614+091	no	4–33	103 ± 6	135 ± 4	K10
SLX 1735–269	yes	6	76 ± 2	73 ± 3	G08
SAX J1747.0–2853	yes	5.0 ± 0.1	537 ± 5	531 ± 5	G08
EXO 1745–248	yes	6.0 ± 0.1	55 ± 2	130 ± 3	G08
4U 1820–30	no	5.5 ± 0.2	840 ± 4	698 ± 10	G08
SAX J1828.5–1037	yes	4.3 ± 1.6	18 ± 2	30 ± 2	C02
4U 1850–086 (1st)	yes	5.9 ± 0.9	12 ± 3	22 ± 4	This work
(2nd)			7 ± 5	16 ± 3	
Aql X-1	yes	8.9 ± 1.5	956 ± 13	338 ± 4	G08

* The peak bolometric flux of the normal bursts

† The ten-day average fluxes in the 2–20 keV band.

‡ The references are K10: Kuulkers et al. 2010, G08: Galloway et al. 2008, C02: Cornelisse et al. 2002c.

Shirasaki, Y., Kawai, N., Yoshida, A., et al. 2003, in Society of Photo-Optical Instrumentation Engineers (SPIE) Conference Series, Vol. 4851, X-Ray and Gamma-Ray Telescopes and Instruments for Astronomy., ed. J. E. Truemper & H. D. Tananbaum, 1310–1319

Strohmayer, T. E. & Brown, E. F. 2002, ApJ, 566, 1045

Strohmayer, T. E. & Markwardt, C. B. 2002, ApJ, 577, 337

Sugizaki, M., Mihara, T., Serino, M., et al. 2011, PASJ, 63, 635

Suzuki, M., Arimoto, M., Ishikawa, N., et al. 2006, Nuovo Cimento B Serie, 121, 1593

Wijnands, R. 2001, ApJL, 554, L59

Table 3. The spectral parameters of the bursts.

Name	MJD*	kT_{bb}^{\dagger} (keV)	F_{bb}^{\ddagger} (10^{-8} ergs cm $^{-2}$ s $^{-1}$)	N_{H}^{\S} (10^{22} cm $^{-2}$)	χ^2 (DoF) $^{\parallel}$
4U 0614+091				—	83.62 (84)
	56964.63	$1.9^{+0.2}_{-0.2}$	$3.3^{+0.4}_{-0.4}$		
	56964.69	$1.5^{+0.2}_{-0.2}$	$1.6^{+0.3}_{-0.3}$		
	56964.76	$1.6^{+0.3}_{-0.3}$	$1.9^{+0.4}_{-0.4}$		
	56964.82	$1.8^{+0.8}_{-0.5}$	$1.3^{+0.6}_{-0.4}$		
	56964.89	$1.8^{+0.5}_{-0.5}$	$1.0^{+0.4}_{-0.3}$		
SLX 1735–269				—	24.43 (29)
	56267.15	$2.8^{+0.3}_{-0.3}$	$4.4^{+0.7}_{-0.6}$		
	56267.15	$1.9^{+0.8}_{-0.5}$	$0.5^{+0.2}_{-0.2}$		
SAX J1747.0–2853				10	131.79 (143)
	55605.58	$2.0^{+0.3}_{-0.3}$	$1.5^{+0.2}_{-0.2}$		
	55605.65	$1.5^{+0.3}_{-0.3}$	$1.0^{+0.2}_{-0.2}$		
	55605.71	$1.4^{+0.5}_{-0.4}$	$0.6^{+0.2}_{-0.2}$		
	55605.77–55605.84	$1.2^{+0.4}_{-0.4}$	$0.5^{+0.2}_{-0.2}$		
EXO 1745–248					
	55858.56	$2.2^{+0.3}_{-0.3}$	$1.2^{+0.2}_{-0.2}$	—	8.93 (16)
	55858.62	$1.7^{+0.5}_{-0.4}$	$0.6^{+0.2}_{-0.2}$	—	6.09 (8)
	55858.75	$1.7^{+0.3}_{-0.2}$	$0.5^{+0.1}_{-0.1}$	—	5.68 (6)
	55858.82–55858.88	$1.6^{+0.5}_{-0.3}$	$0.3^{+0.1}_{-0.1}$	—	3.59 (4)
	55858.94–55859.14	$1.2^{+0.3}_{-0.3}$	$0.1^{+0.03}_{-0.03}$	—	3.32 (4)
4U 1820–30				—	223.29 (203)
	55272.72	$3.0^{+0.2}_{-0.2}$	$5.3^{+0.5}_{-0.5}$		
SAX J1828.5–1037					
	55877.36	$2.7^{+0.9}_{-0.6}$	$0.9^{+0.3}_{-0.3}$	4.1	3.03 (5)
	55877.43	$1.3^{+0.3}_{-0.3}$	$0.4^{+0.1}_{-0.1}$	4.1	3.11 (5)
	55877.49–55877.55	$1.5^{+0.3}_{-0.3}$	$0.2^{+0.1}_{-0.1}$	4.1	5.53 (6)
4U 1850–086 (2nd)					
	57151.39	$2.6^{+0.1}_{-0.1}$	$7.8^{+0.5}_{-0.5}$	—	90.49 (98)
	57151.46	$0.7^{+0.3}_{-0.2}$	$0.2^{+0.1}_{-0.1}$	—	0.82 (3)
Aql X-1				—	173.15 (188)
	56493.30	$1.8^{+0.2}_{-0.2}$	$2.0^{+0.3}_{-0.3}$		
	56493.37	$1.9^{+0.3}_{-0.3}$	$1.2^{+0.3}_{-0.3}$		
	56493.43	$1.6^{+0.6}_{-0.4}$	$0.5^{+0.2}_{-0.2}$		
	56493.50	$1.4^{+0.4}_{-0.3}$	$0.6^{+0.2}_{-0.2}$		
	56493.56	$1.2^{+0.4}_{-0.3}$	$0.5^{+0.2}_{-0.2}$		
	56493.63	$1.9^{+1.6}_{-1.2}$	$0.5^{+0.3}_{-0.2}$		
	56493.69	$2.3^{+1.1}_{-1.1}$	$0.4^{+6.3}_{-0.2}$		
	56493.76	$1.0^{+0.5}_{-0.4}$	$0.3^{+0.2}_{-0.2}$		

* The center time of the scan in Modified Julian Date

 † The blackbody temperature of the spectrum ‡ The bolometric flux of the spectrum § The hydrogen column density $^{\parallel}$ The χ^2 and the degrees of freedom of the fit

Table 4. The properties of the bursts studied in this paper.

Name	F_{obs} (10^{-8} ergs cm $^{-2}$ s $^{-1}$)	F_{max}	τ_{LB} (hour)	d (kpc)	E_{b}^* (10^{41} ergs)	first burst † (day)
4U 0614+091	$3.3^{+0.4}_{-0.4}$	4.0	5.2	3 (A,B)	6.7 ± 0.8 (+1.4)	—
SLX 1735–269	$4.4^{+0.7}_{-0.6}$	32	0.77	7.3 (C)	7.8 ± 1.2 (+49)	—
SAX J1747.0–2853	$1.5^{+0.2}_{-0.2}$	1.9 (6.9) ‡ (D)	4.2	9 (E)	22 ± 2.9 (+5.4)	≤ 25 (F)
EXO 1745–248	$1.2^{+0.2}_{-0.2}$	1.5	4.2	5.5 (G)	6.6 ± 1.1 (+1.7)	—
				6.9 (H)	10 ± 1.7 (+2.6)	
4U 1820–30	$5.3^{+0.5}_{-0.5}$	110	0.5 ± 0.1 (I)	7.9 (H)	7.1 ± 2.1 (+146)	≤ 1549 (this work)
SAX J1828.5–1037	$0.9^{+0.3}_{-0.3}$	1.7	2.3	< 6.2 (J)	$< 3.4 \pm 1.1$ (+3.2)	—
4U 1850–086 (1st)	10.7 ± 0.9 (K)	—	0.27 (K)	6.9 (H)	5.9 ± 0.5 (+0)	≤ 425 (this work)
(2nd)	$7.8^{+0.5}_{-0.5}$	13	0.71		11 ± 0.7 (+7.8)	≤ 186 (this work)
Aql X-1	$2.0^{+0.3}_{-0.3}$	2.6	4.3	5.0 (C)	9.3 ± 1.4 (+2.7)	≤ 389 (this work)

* The radiated burst energy with statistic (systematic) error.

The systematic error is due to the uncertainty of the peak flux.

† The time of the first X-ray burst after the sample event.

‡ The number in the parentheses is the observed peak flux by INTEGRAL with bolometric correction (see text).

References are (A) Brandt et al. 1992, (B) Kuulkers et al. 2010, (C) Galloway et al. 2008,

(D) Chenevez et al. (2011), (E) Natalucci et al. 2000, (F) Linares et al. 2011, (G) Ortolani et al. 2007,

(H) Harris 2010, (I) in't Zand et al. 2011, (J) Cornelisse et al. 2002c, (K) in't Zand et al. 2014.